Self-Assembled Monolayers Containing Terminal Mono-, Bis-, and Tris-nitrilotriacetic Acid Groups: Characterization and Application

ARTICLE *in* LANGMUIR · JUNE 2008

Impact Factor: 4.46 · DOI: 10.1021/la703709a · Source: PubMed

Self-Assembled Monolayers Containing Terminal Mono-, Bis-, and Tris-nitrilotriacetic Acid Groups: Characterization and Application

Ramūnas Valiokas,*[,§,‡,†] Goran Klenkar,[§] Ali Tinazli,[‡] Annett Reichel,[‡] Robert Tampé,*[,‡] Jacob Piehler,*[,‡] and Bo Liedberg[§]

Department of Functional Nanomaterials, Institute of Physics, Savanoriu; 231, LT-02300 Vilnius, Lithuania, Division of Molecular Physics, Department of Physics, Chemistry and Biology, Linköping University, 58183 Linköping, Sweden, and Institute of Biochemistry, Johann Wolfgang Goethe-University, Max-von-Laue-Strasse 9, 60438 Frankfurt, Germany

Received November 27, 2007. In Final Form: January 22, 2008

We have undertaken a structural and functional study of self-assembled monolayers (SAMs) formed on gold from a series of alkylthiol compounds containing terminal multivalent chelators (MCHs) composed of mono-, bis-, and tris-nitrilotriacetic acid (NTA) moieties. SAMs were formed from single-component solutions of the mono-, bis-, and tris-NTA compounds, as well as from mixtures with a tri(ethylene glycol)-terminated alkylthiol (EG_3). Contact angle goniometry, null ellipsometry, and infrared spectroscopy were used to explore the structural characteristics of the MCH SAMs. Ellipsometric measurements show that the amount of the MCH groups on surfaces increases with increasing mol % of the MCH thiols in the loading solution up to about 80 mol %. We also conclude that mixed SAMs, prepared in the solution composition regime 0−30 mol % of the MCH thiols, consist of a densely packed alkyl layer, an amorphous ethylene glycol layer, and an outermost layer of MCH groups exposed toward the ambient. Above 30 mol %, a significant degree of disorder is observed in the SAMs. Finally, functional evaluation of the three MCH SAMs prepared at 0−30 mol% reveals a consistent increase in binding strength with increasing multivalency. The tris-NTA SAM, in particular, is enabled for stable and functional immobilization of a His_6-tagged extracellular receptor subunit, even at low chelator surface concentrations, which makes it suitable for applications when a low surface density of capturing sites is desirable, e.g., in kinetic analyses.

Introduction

During the past decade, protein-compatible surface architectures have emerged as a highly promising area of science and technology. They are believed to mark the beginning of a new development in biological and biomedical sciences, opening tremendous possibilities to study the human proteome, which consists of ∼25 000 different proteins undergoing various post-translational modifications.[1] Natural and engineered proteins are considered to become functional building blocks primarily because of the huge variation in specific functions developed by the evolution process. The formation of functional and stable protein assemblies and their nanoscale characteristics on solid surfaces, however, remains a challenge. New chemical tools and supramolecular strategies have to be developed to allow precise positioning of single protein molecules on micro- and nanostructured solid surfaces for biochip and device fabrication.

One promising strategy in this regard is to employ multivalent interactions.[2−6] They have proven to be particularly effective for immobilizing biomolecular recognition systems at interfaces, thus providing an additional degree of multivalency: surface multivalency.[7,8] Such artificial multivalent systems recently have been employed as molecular print boards.[9,10] Moreover, multivalent chelators (MCHs) based on nitrilotriacetic acid (NTA) derivatives have proven powerful and superior in comparison to the monovalent NTA (mono-NTA) derivatives for immobilization of oligohistidine tagged (His-tagged) biomolecules in the presence of Ni(II) ions.[11,12] Also, it has been demonstrated that the MCHs can be synthetically attached to compounds that form self-assembled monolayers (SAMs), another powerful platform to control orientation, surface density, and composition of protein entities on surfaces.[12−14] Previously, mixed SAMs on gold have been assembled from solution mixtures of mono-NTA-terminated thiol compounds and filling molecules,[15−17] or synthesized in situ.[18] However, the recent introduction of multivalent NTA-terminated SAMs,[12] which allow us to control the stability of the interaction between the His-tagged protein and surface at molecular level, extend the application range. In particular, they

* Corresponding author. E-mail: valiokas@ar.fi.lt, phone: +370 5 2661640, fax +370 5 2602317. Corresponding authors regarding concept and synthesis of NTA-terminated alkylthiols. Robert Tampé, E-mail: tampe@em.uni-frankfurt.de, phone: +49 69 798 29475, fax: +49 69 798 29495. Jacob Piehler, E-mail: j.piehler@em.uni-frankfurt.de, phone: +49 69 798 29468, fax: +49 69 798 29495.

† Institute of Physics.

‡ Linköping University.

§ Johann Wolfgang Goethe-University.

(1) Southan, C. *Proteomics* **2004**, *4*, 1712−1726.

(2) Badjic, J. D.; Nelson, A.; Cantrill, S. J.; Turnbull, W. B.; Stoddart, J. F. *Acc. Chem. Res.* **2005**, *38*, 723−732.

(3) Kiessling, L. L.; Gestwicki, J. E.; Strong, L. E. *Angew. Chem., Int. Ed.* **2006**, *45*, 2348−2368.

(4) Kitov, P. I.; Sadowska, J. M.; Mulvey, G.; Armstrong, G. D.; Ling, H.; Pannu, N. S.; Read, R. J.; Bundle, D. R. *Nature* **2000**, *403*, 669−672.

(5) Mammen, M.; Choi, S. K.; Whitesides, G. M. *Angew. Chem., Int. Ed.* **1998**, *37*, 2755−2794.

(6) Rao, J. H.; Lahiri, J.; Isaacs, L.; Weis, R. M.; Whitesides, G. M. *Science* **1998**, *280*, 708−711.

(7) Huskens, J. *Curr. Opin. Chem. Biol.* **2006**, *10*, 537−543.

(8) Mulder, A.; Auletta, T.; Sartori, A.; Del Ciotto, S.; Casnati, A.; Ungaro, R.; Huskens, J.; Reinhoudt, D. N. *J. Am. Chem. Soc.* **2004**, *126*, 6627−6636.

(9) Ludden, M. J. W.; Mulder, A.; Tampe, R.; Reinhoudt, D. N.; Huskens, J. *Angew. Chem., Int. Ed.* **2007**, *46*, 4104−4107.

(10) Ludden, M. J. W.; Reinhoudt, D. N.; Huskens, J. *Chem. Soc. Rev.* **2006**, *35*, 1122−1134.

(11) Lata, S.; Reichel, A.; Brock, R.; Tampe, R.; Piehler, J. *J. Am. Chem. Soc.* **2005**, *127*, 10205−10215.

(12) Tinazli, A.; Tang, J. L.; Valiokas, R.; Picuric, S.; Lata, S.; Piehler, J.; Liedberg, B.; Tampe, R. *Chem.—Eur. J.* **2005**, *11*, 5249−5259.

(13) Klenkar, G.; Valiokas, R.; Lundstrom, I.; Tinazli, A.; Tampe, R.; Piehler, J.; Liedberg, B. *Anal. Chem.* **2006**, *78*, 3643−3650.

(14) Valiokas, R.; Klenkar, G.; Tinazli, A.; Tampe, R.; Liedberg, B.; Piehler, J. *ChemBioChem* **2006**, *7*, 1325−1329.

(15) Sigal, G. B.; Bamdad, C.; Barberis, A.; Strominger, J.; Whitesides, G. M. *Anal. Chem.* **1996**, *68*, 490−497.

(16) Liley, M.; Keller, T. A.; Duschl, C.; Vogel, H. *Langmuir* **1997**, *13*, 4190−4192.

(17) Wegner, G. J.; Lee, N. J.; Marriott, G.; Corn, R. M. *Anal. Chem.* **2003**, *75*, 4740−4746.

(18) Lee, J. K.; Kim, Y. G.; Chi, Y. S.; Yun, W. S.; Choi, I. S. *J. Phys. Chem. B* **2004**, *108*, 7665−7673.

10.1021/la703709a CCC: $40.75
Published on Web 04/08/2008

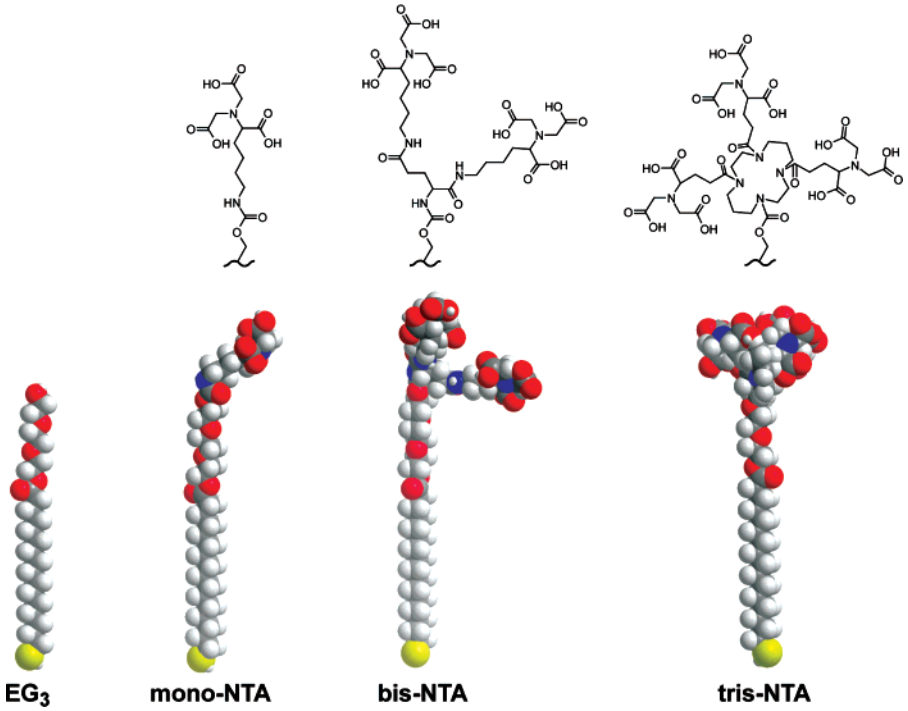

Figure 1. Space-filling models and chemical structures of the filling compound (EG_3) and the mono- and multivalent chelator derivatives used to form self-assembled monolayers on gold.

are interesting for multiplexed protein immobilization and design of functional protein micro- and nanopatterns.[14,19]

We report herein a systematic structural and functional study of SAMs formed on gold from a series of alkylthiol compounds containing mono-, bis-, and tris-NTA moeities (Figure 1) mixed with a tri(ethylene glycol)-terminated alkylthiol (EG_3) at different compositions. We analyzed the SAMs using contact angle goniometry, null ellipsometry, and infrared spectroscopy in order to explore how the structural characteristics of such complex assemblies can be controlled and manipulated. The specific vs nonspecific binding characteristics as well as the stability of the immobilized proteins were further analyzed by surface plasmon resonance (SPR). Finally, imaging SPR operating in ellipsometric mode was utilized to follow, in parallel, the protein association/dissociation characteristics to/from mixed MCH SAM microspots. Thus, the functional properties of density arrays of mono-, bis-, and tris-NTA SAMs are demonstrated, keeping in mind their potential applications in proteomics and nanobiotechnology.

Experimental Section

Synthesis of Metal-Chelating Thiol Compounds. The synthesis of mono-NTA and bis-NTA thiols was recently described in detail by Tinazli et al.[12] The synthesis of the tris-NTA thiols is outlined below and in Scheme 1.

16-Acetylsulfanyl-hexadecanoic Acid EG_3 (3). 16-Acetylsulfanyl-hexadecanoic acid EG_3 (AcS-HD-EG_3) was synthesized from 16-mercaptohexadecanoic acid (**1**) via 16-acetylsulfanyl-hexadecanoic acid (AcS-HD) (**2**) as described previously.[12]

Tris-NTA (OtBu) (4). Tris-NTA (OtBu) was synthesized as described previously.[11]

16-Acetylsulfanyl-hexadecanoic Acid EG_3 Tris-NTA (OtBu) (5). $(COCl_2)_3$ (0.32 g, 1.08 mmol) was added to a solution of AcS-HD-EG_3 (0.5 g, 1.08 mmol) (**3**) in dry CH_2Cl_2. The reaction flask was purged with nitrogen, and diisopropylethylamine (DIPEA) (0.42 g, 3.24 mmol) was added. The reaction mixture was stirred for 4 h at room temperature. The solvent was evaporated and reaction mixture dried in high vacuum. The mixture was dissolved in dry CH_2Cl_2, and tris-NTA-OtBu (1.56 g, 1.08 mmol) (**4**) and DIPEA (0.42 g, 3.24 mmol) were added. The reaction mixture was stirred overnight at room temperature. The reaction mixture was diluted with CH_2Cl_2 and washed three times with water. The organic phase was dried over Na_2SO_4, and the solvent was evaporated. The crude product AcS-HD-tris-NTA (OtBu) (**10**) was purified by silica chromatography using ethyl acetate (EA) as eluent. Thin layer chromatography (TLC): R_f = 0.3 (EA). Yield: 0.90 g (43%). Analytical data calculated for $C_{98}H_{173}N_7O_{28}S$: MW 1929.52. MS: 1928.8 (ESI^+) (M^+Na^+).

16- Mercapto-hexadecanoic Acid EG_3 Tris-NTA (OtBu) (6). Hydrazinium acetate (0.57 g, 6.16 mmol) was added to a solution of AcS-HD-EG_3-tris-NTA (OtBu) (0.9 g, 0.47 mmol) (**5**) in dimethylformamide (25 mL). The reaction flask was purged with nitrogen. The reaction mixture was stirred for 48 h at room temperature. The reaction mixture was diluted with CH_2Cl_2 and washed (three times) with water. The organic phase was dried over Na_2SO_4, and the solvent was evaporated. The crude product HS-HD-EG_3-tris-NTA (OtBu) (**6**) was purified by chromatography using ethyl acetate as eluent. TLC: R_f = 0.3 (ethyl acetate). Yield: 0.54 g (60%). Analytical data calculated for $C_{96}H_{171}N_7O_{27}S$: MW 1887.48. MS: 1887.2 (ESI^+).

16- Mercapto-hexadecanoic Acid EG_3 Tris-NTA (7). A mixture of trifluoroacetic acid (3.9 mL), ethanedithiol (1 mL), and water (0.1 mL) was added to HS-HD-EG_3-tris-NTA (OtBu) (0.54 g, 0.29 mmol) (**6**). The reaction flask was purged with nitrogen. The reaction mixture was stirred for 4 h at room temperature. Subsequently solvent was evaporated and the reaction mixture dried in high vacuum. The rest was dissolved in diethyl ether and precipitated with petroleum ether. Supernatant was removed, and the procedure was repeated twice time. Crystals of HS-HD-EG_3-tris-NTA (**7**) were dried in high vacuum overnight. Yield: 0.138 g (34%). Analytical data calculated for $C_{60}H_{99}N7O_{27}S$: MW 1381.63, MS: 1403.02 (ESI^+) (MNa^+).

Preparation of SAMs. The details for preparation of the gold substrates in ultrahigh vacuum have been reported elsewhere,[20,21] and these substrates were used for contact angle goniometry,

(19) Tinazli, A.; Piehler, J.; Beuttler, M.; Guckenberger, R.; Tampe, R. *Nat. Nanotechnol.* **2007**, *2*, 220−225.

(20) Bertilsson, L.; Liedberg, B. *Langmuir* **1993**, *9*, 141−149.

(21) Valiokas, R.; Svedhem, S.; Ostblom, M.; Svensson, S. C. T.; Liedberg, B. *J. Phys. Chem. B* **2001**, *105*, 5459−5469.

Scheme 1. Synthesis of the Tris-NTA Thiol (7)[a]

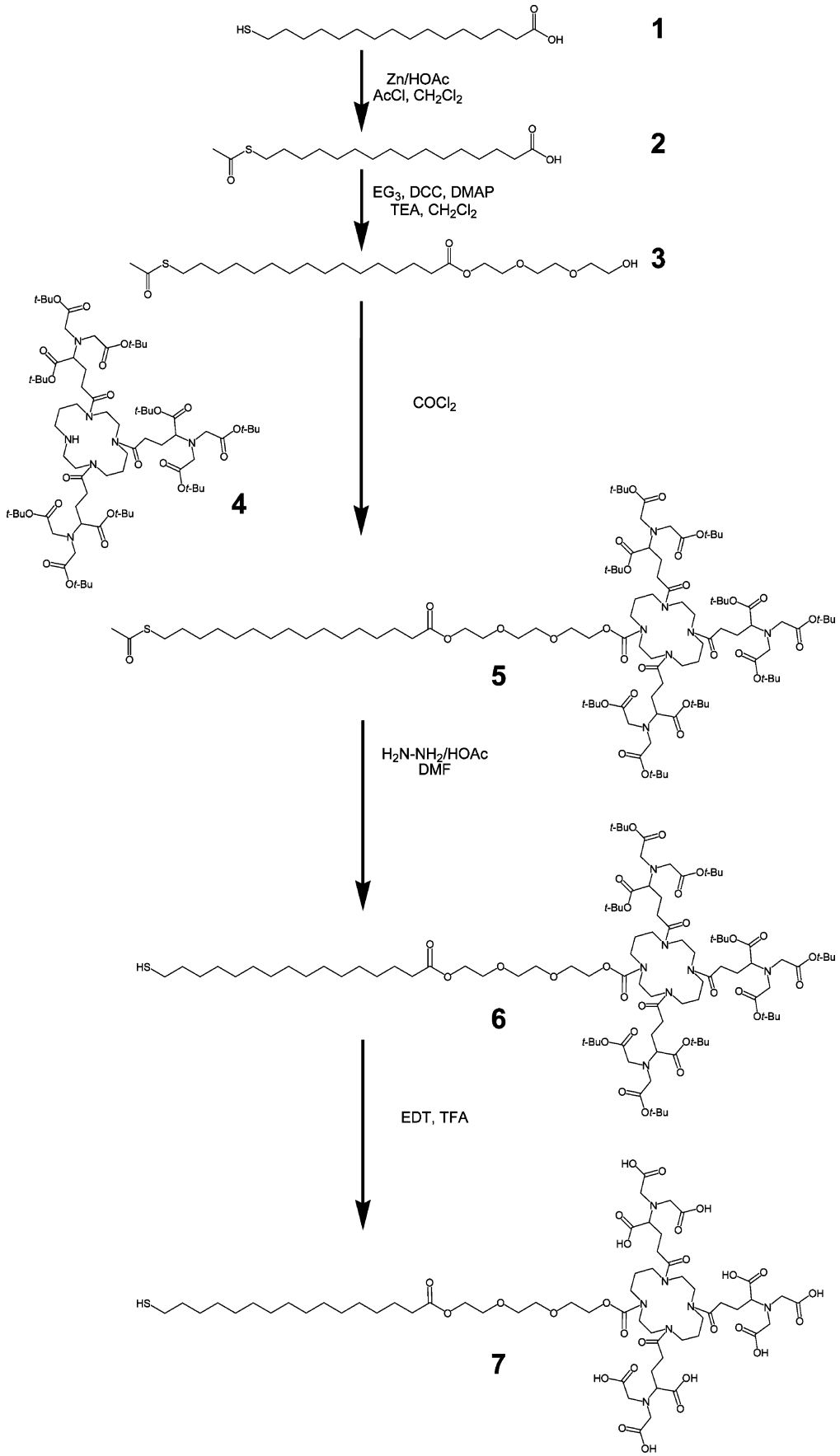

[a] Abbreviations: HOAc, acetic acid; AcCl, acetyl chloride; DDC, dicyclohexylcarbodiimide; TEA, triethylamine; DMF, dimethylformamide; EDT, ethanedithiol; TFA, trifluoracetic acid; DMAP, dimethylaminopyridine.

ellipsometry, and infrared reflection−absorption spectroscopy. Briefly, gold surfaces for SAM formation were prepared in ultrahigh vacuum by e-beam evaporation of 25 Å titanium adhesion layer followed by 2000 Å of gold on standard (100)-silicon wafers. Before the evaporation, they were cut and cleaned in a 5:1:1 mixture of MilliQ water, 25% hydrogen peroxide, and 30% ammonia for 5 min at 85 °C, followed by extensive rinsing in MilliQ water. The same cleaning procedure was used at least twice also for the prepared gold surfaces before soaking them into the thiol solutions. For SPR (Biacore) experiments gold-coated glass substrates were obtained from Biacore-GE, Uppsala, Sweden. For imaging SPR measurements 300 Å of gold was evaporated onto SF10 glass substrates (Schott, Germany), precoated with 10 Å of titanium.

In our previous study, we formed mixed SAMs of mono and bis-NTA from solutions of these molecules in acetonitrile and THF (tetrahydrofuran), respectively.[12] However, in this study we changed the solvent to ethanol because of its better suitability for the piezoelectric ink-jet printing process (considering also the health hazards of THF and acetonitrile). Thus, for SAM formation, fresh solutions of the alkyl thiols were prepared at different mixing ratios (EG_3 mixed with either mono-NTA, bis-NTA, or tris-NTA thiol, respectively) in 99.5% ethanol, keeping a total thiol concentration of 20 μM. After the incubation for at least 24 h, the SAM samples were washed for 3−5 min in an ultrasonic bath and rinsed extensively in EtOH, blown dry with nitrogen gas, and then immediately used for analysis. For functional studies, they were also preconditioned in buffer.

Contact Angle Goniometry. Contact angles were measured with a Ramé-Hart NRL 100 goniometer (Ramé-Hart, Mountain Lakes, USA) using MilliQ water, without control of the ambient humidity. Taking the high surface energy of the hydrophilic surfaces into account, one measurement of the advancing and the receding contact angle was performed per sample. At least three different samples were measured for each mixing ratio and each MCH thiol, respectively.

Ellipsometry. Single-wavelength ellipsometry was used for thickness determination (AutoEL, Rudolph Research, Flanders, USA). The average refractive index of the clean gold substrate, obtained prior to the incubation, were used as input values in the determination of SAM thickness using a three-layer model "ambient/organic film/ gold", assuming an isotropic, transparent organic layer with the refractive index of $n = 1.5$.[22] The film thickness was calculated by averaging values from three different spots on at least four samples for each SAM.

Infrared Reflection−Absorption Spectroscopy (IRAS). The reflection−absorption spectra were recorded at room temperature on a Bruker IFS 66 system (Bruker Optik GmbH, Bremen, Germany), equipped with a grazing angle infrared reflection accessory aligned at 85° and a liquid-nitrogen-cooled MCT detector. The measurement chamber was continuously purged with nitrogen gas during the measurements. The acquisition time was around 10 min at 2 cm^{-1} resolution, and three-term Blackmann−Harris apodization function was applied to the interferograms before Fourier transformation. A spectrum of a deuterated hexadecanethiolate ($HS(CD_2)_{15}CD_3$) on gold was used as the reference R_o.

SPR Analysis. Unmodified SPR-chips (Biacore, Sweden) were cleaned and treated in the same way as the other substrates. Experiments were performed on a Biacore 2000 (Biacore, Sweden) under a continuous flow of 10 μL/min in HEPES−buffered saline (10 mM HEPES pH 7.4, 150 mM NaCl) supplemented with 0.015% (v/v) Tween 20 (HBS-P). Specific and nonspecific binding to the MCH surfaces was assessed with the ectodomain of the type I interferon receptor subunit ifnar2 fused to a C-terminal hexahistidine tag (ifnar2- His_6, 500 nM). To verify the functionality of immobilized ifnar2- His_6, the ligand interferon α2 (IFNα2) was injected at a concentration of 100 nM. The expression and purification of the proteins have been described elsewhere.[23−25] Prior to protein loading, the chips were conditioned by a 3.5 min injection of 200 mM ethylenedinitrilotetraacetic acid (EDTA) pH 7.5 and the NTA chelators were subsequently loaded by an injection of 100 mM $NiCl_2$ (3.5 min). Nonspecific protein binding to the chips was evaluated by excluding the $NiCl_2$ loading step and injecting ifnar2- His_6 in the presence of 1 mM EDTA (in order to remove transition metal ion contaminants). The chips were regenerated with a 2 min injection of 1 M imidazole. For studying differences in protein elution from the different chips, 2 min sequential injections of imidazole in increasing concentrations (2, 5, 10, 20, and 40 mM) were carried out after protein immobilization.

Microarray Experiments. Chips were manufactured, and biomolecular interactions were monitored on them as described previously.[13] In brief, the array was made by dispensing ethanolic mixtures of mono-, bis-, and tris-NTA in different ratios with EG_3 on a surface with microcontact printed hydrophobic barriers. Before being docked in the instrument, the chip was incubated in 1 mg/mL bovine serum albumin (BSA) for 10 min to passivate hydrophobic regions of the chip. The instrument was an imaging null-ellipsometer (EP^3, Nanofilm, Germany) equipped with a surface plasmon resonance (SPR) cell, according to the Kretschmann configuration,[26] and connected to a ~10 μL flow cell. SPR images were recorded as the reflectance of p-polarized light, and difference images were constructed by subtracting an image after an event with the one previously. Intensity is directly proportional to adsorbed mass under the used setup. Continuous monitoring of biomolecular interactions was done by recording the ellipsometric angle Δ over time for relevant regions of interest of the chip. Δ is inversely proportional to adsorbed mass under the used setup. Maltose binding protein fused to a C-terminal decahistidine tag (MBP-His_{10}) was used to study protein immobilization and elution by imidazole on the arrayed multivalent chelator mixtures. The cloning, expression, and purification of His-tagged MBP has been described elsewhere.[27] A continuous flow system was used at 20 μL/min and HBS-P was used as buffer. Sensorgrams have been corrected for background responses by subtraction with the signal from the BSA-covered frames.

Results and Discussion

General Properties of Single Component SAMs. We have studied, in detail, the formation of SAMs on gold from solutions containing EG_3 and analogous compounds.[21,28,29] This particular EG_3 compound self-assembles into a well-defined structure, with the alkyls in an extended all-trans conformation indicated by the alkyl CH_2 asymmetric (ν_a) and symmetric (ν_s) stretching modes at 2918 and 2850 cm^{-1}, respectively.[30] The $\nu_a(CH_2)$ and $\nu_s(CH_2)$ modes of the terminal oligo(ethylene glycol)-OEG segments appear as broad features at around 2950 cm^{-1} and 2879 cm^{-1}, respectively. These spectral positions and the absence of a strong $\nu_a(CH_2)$ peak at close to 2890 cm^{-1}, Figure 2a, suggest that the OEG segments do not relax in the expected helical conformation, as was observed for the corresponding methoxy-EG_3 analogue.[31] Instead, the OEG portion of the EG_3 SAM under investigation seems to adopt an amorphous-like conformation. This assignment is confirmed by the presence of a broad peak originating from the skeletal C−O, C−C modes at 1137 cm^{-1}, Figure 2b. Thus, the EG_3 SAM is composed of an ordered alkyl layer and a

(22) Ulman, A., *An Introduction to Ultrathin Organic Films from Langmuir-Blodgett to Self-Assembly*; Academic Press: San Diego, CA, 1991.

(23) Lamken, P.; Lata, S.; Gavutis, M.; Piehler, J. *J. Mol. Biol.* **2004**, *341*, 303−318.

(24) Piehler, J.; Roisman, L. C.; Schreiber, G. *J. Biol. Chem.* **2000**, *275*, 40425−40433.

(25) Piehler, J.; Schreiber, G. *J. Mol. Biol.* **1999**, *289*, 57−67.

(26) Raether, H. *Surface Plasmons on Smooth and Rough Surfaces and on Gratings*; Springer-Verlag: Berlin, 1988; Vol. 111, p 136

(27) Lata, S.; Piehler, J. *Anal. Chem.* **2005**, *77*, 1096−1105.

(28) Benesch, J.; Svedhem, S.; Svensson, S. C. T.; Valiokas, R.; Liedberg, B.; Tengvall, P. *J. Biomater. Sci., Polym. Ed.* **2001**, *12*, 581−597.

(29) Valiokas, R.; Ostblom, M.; Svedhem, S.; Svensson, S. C. T.; Liedberg, B. *J. Phys. Chem. B* **2002**, *106*, 10401−10409.

(30) Porter, M. D.; Bright, T. B.; Allara, D. L.; Chidsey, C. E. D. *J. Am. Chem. Soc.* **1987**, *109*, 3559−3568.

(31) Harder, P.; Grunze, M.; Dahint, R.; Whitesides, G. M.; Laibinis, P. E. *J. Phys. Chem. B* **1998**, *102*, 426−436.

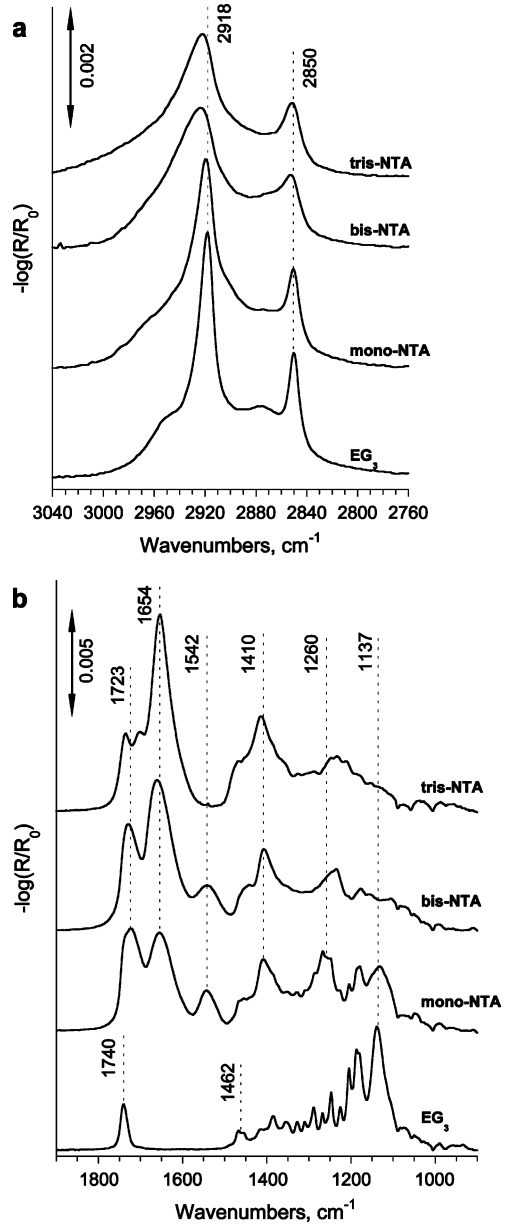

Figure 2. Infrared RA spectra of 100% SAMs formed from the four compounds used in this study: (a) the CH stretching region and (b) the fingerprint region.

disordered, amorphous-like, outermost OEG layer. Although it is known that OEG-SAMs with helical conformation display superior protein rejecting properties, as compared to the all-trans and amorphous conformations,[31,32] the present EG_3 molecules seem to provide a background coating with sufficiently low levels of nonspecific binding for the proteins used in this study (see below). The typical signature of the ester group found in the fingerprint region is the ν(C═O) mode at 1740 cm^{-1}. Other major features in the fingerprint region are the burst of sharp peaks between 1435 and 1160 cm^{-1}. These sharp features, the progression peaks, are attributed to the presence of highly ordered alkyls normally found in ester-linked alkylthiol SAMs. Also, the doublet found at 1468/1455 cm^{-1}, which corresponds to CH_2 scissoring modes, is typical for highly ordered alkylthiol SAMs.

Our IRAS data clearly shows that the introduction of mono-, bis-, and tris-NTA groups affects the conformation of the alkyl portion of the SAMs. These bulky groups interact laterally upon formation of the SAMs on the surface, and a densely packed assembly of alkyl chains in an extended all-trans conformation is no longer possible. For example, for mono-NTA, the symmetric and asymmetric C−H stretching peaks appear at 2919 cm^{-1} and 2851 cm^{-1}, respectively, and the FWHM of the asymmetric peak increases as compared to the FWHM of the same peak in the EG_3-SAM. These observations are all indicative of an increasing presence of gauche conformers in the alkyl portion.[30] Moreover, the alkyls appear to be even more disordered in the bis- and tris-NTA SAMs (Figure 2b), as demonstrated by the transformation of the methylene ν_a peaks into broad and asymmetric features with maxima at around 2925 and 2923 cm^{-1}, respectively. The remarkable variation in the appearance of these peaks is most likely due to the differences in chemical structure of the three MCH moieties. For example, the number of non-alkylthiol CH_2 groups and their packing and local chemical environment vary considerably for the mono-, bis-, and tris-NTA tail groups.

The low-frequency region, Figure 2b, contains several peaks that can be assigned to the terminal MCH groups. First of all, a strong carboxyl ν(C═O) peak is found between 1723 and 1739 cm^{-1}. The slight variation in the peak position suggests that the terminal COOH group experiences different intra- and intermolecular interactions in the three MCH SAMs. Also, a contribution from the ν(C−O) mode can be found as a broad feature with a maximum centered near 1260 cm^{-1} (mono-NTA) and near 1210 cm^{-1} for bis- and tris-NTA. Second, a significant population of the terminal carboxylic groups is deprotonated, as indicated by strong asymmetric carboxylate ν_a peaks at 1654 cm^{-1} (mono-NTA), 1659 cm^{-1} (bis-NTA), 1645 cm^{-1} (tris-NTA), respectively. The corresponding symmetric carboxylate ν_s peak appears at around 1410 cm^{-1}. The differences in the relative intensity ratio between the above-mentioned carboxyl and carboxylate peaks in the spectra, Figure 2b, suggest different protonation states for the three MCH groups. This is not surprising keeping in mind the structural differences between the molecules under investigation. For example, mono- and bis-NTA are coupled to the ethylene glycol spacer via amide moieties, whereas tris-NTA is based on a carbamide ring structure, differences that potentially affect the formation of intra- and intrermolecular hydrogen bonds.

The other distinctive features found in the fingerprint region of the RA spectra of mono- and bis-NTA SAMs is the amide II peak at 1542 cm^{-1}, whereas the amide I peak overlaps with the strong carboxylic acid/carboxylate ν(C═O) peaks discussed above. We note also a different set of peaks in the 1800−1600 cm^{-1} region of the tris-NTA spectrum, Figure 2b. A new peak appears near 1700 cm^{-1} which is tentatively attributed to the C═O group near the central ring structure of the compound, see Scheme 1. Also evident is that the OEG skeletal modes and the ester ν(C−O) peaks still can be identified in the mono-NTA spectrum. These peaks broaden in the bis- and tris-NTA spectra and disappear in a broad background, which again is consistent with an increasing disorder in the supporting alkyl- and OEG chains of the SAM. Thus, the IRAS data allows us to conclude that the bulky and charged NTA groups hinder formation of ordered MCH SAMs, as indicated by distinctive changes in IR peaks from the alkyl-ester-OEG portions of the constituent molecules.

Mixed SAMs. The above-described set of molecules is further used to design functional assemblies for the analysis of the multivalency-dependent adsorption and elution of His-tagged proteins. Therefore, it is necessary to investigate how different mole fractions of the MCHs in solution influence the composition

(32) Riepl, M.; Ostblom, M.; Lundstrom, I.; Svensson, S. C. T.; van der Gon, A. W. D.; Schaferling, M.; Liedberg, B. *Langmuir* **2005**, *21*, 1042−1050.

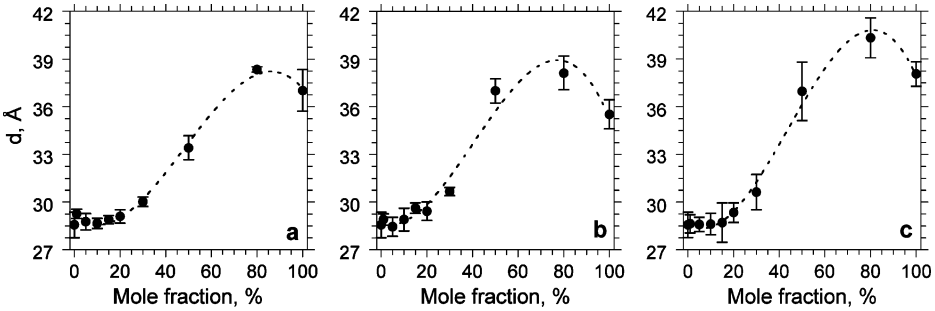

Figure 3. Ellipsometric thickness *d* as a function of the mole fraction of the respective MCH compounds in solution. (a) SAMs prepared with mono-NTA, (b) SAMs prepared with bis-NTA, (c) SAMs prepared with tris-NTA. The error bars are the standard deviation and at least three samples were investigated for each mole fraction. The fitted dashed curves should be regarded as guide lines for the eye.

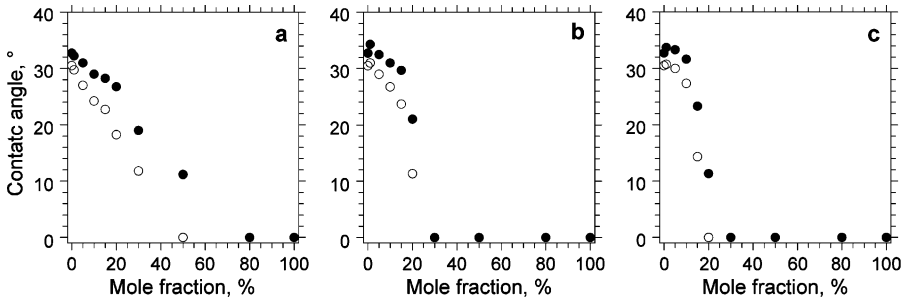

Figure 4. Contact angles of SAMs as a function of the mole fraction of the respective NTA compound in solution. The filled symbols represent the advancing contact angle and the unfilled the receding contact angles. (a) SAMs prepared with mono-NTA, (b) SAMs prepared with bis-NTA, (c) SAMs prepared with tris-NTA. The maximum error is ± 2° and at least three samples were investigated for each point.

and conformation of mixed and EG_3 and mono-, bis-, and tris-NTA-terminated SAMs on gold. We concentrate our efforts on the low concentration range 0−30 mol %, as this range corresponds to the surface concentrations of the MCH that are optimal in terms of binding to the His-tags of the proteins (see below).

The formation of mixed MCH SAMs was investigated by ellipsometry, contact angle goniometry, and IRAS. Figure 3 shows the dependence of the effective thickness, *d*, of the SAM on the mole fraction of the MCH thiols in the incubation solution. One can observe a small but monotonic increase in thickness for all three mixed SAMs in the mole fraction range from 0 to 20 mol %. A further increase in the mole fraction of MCH thiols results in a strong increase in the mixed SAM thickness up to a critical value (chelator-dependent), above which the thickness starts to decrease. The general observation is that the presence of a relatively small fraction of EG_3 in the incubation solution (corresponding to MCH mol % values from ∼70 to 90, Figure 3) gives a thickness that is higher than the corresponding thicknesses of the pure (100%) MCH SAMs. This trend is not very common, but has been observed before upon mixing thiols bearing complex and bulky tail groups.[33,34] We attribute the effect to an additional in-plane stabilization of the assembly offered by the small filling EG_3 molecule leading to a more favorable packing, orientation, and presentation of the NTA tail at the ambient/SAM interface and thus to an increase in thickness. For the three mixed SAMs under investigation, it is mono-NTA that displays the slowest growth in thickness with increasing mol %, whereas the corresponding thickness increases more rapidly for bis- and tris-NTA up to the critical mol %. The exact mechanism behind this behavior is not fully understood, but is most likely correlated to the size, polarity, and solubility of the MCH tail and thereby to the kinetics of the overall assembly process. Note also that the measured thicknesses of the mixed bis- and tris-NTA SAMs suffer from larger measurement errors, which suggests a higher sensitivity to the experimental conditions during the SAM formation process.

Measurement of advancing and receding water contact angles provides further information about the presence of the MCHs in the mixed SAMs. Figure 4 shows that this technique is far more sensitive to the presence of the MCHs in the lower mol % range than ellipsometry. The advancing contact angle for the EG_3 SAM is 33°. However, even a small fraction (<10 mol %) of mono-NTA groups in the SAMs gives a visible change in the surface wetting data (note, that no significant changes in SAM thickness were detected by ellipsometry in this range). The advancing contact angles of the mixed mono-NTA/EG_3 SAMs decrease almost linearly over a broad range of 0−80 mol %. Also, the hysteresis increases continuously with the concentration of NTA groups, which is consistent with the continuous increase of the amount of flexible NTA groups on the surface. A similar behavior is observed also for bis-NTA SAM. The major difference for this SAM, however, is that the contact angles decrease abruptly at around 20 mol %. Moreover, for tris-NTA the onset in decrease of the contact angles is observed already on going from 10 to 15 mol %. The surfaces become completely wetting, that is, they appear to be dominated by the hydrophilic NTA groups exposed to the ambient at around 80 mol % for mono-NTA and at about 30 mol % for bis- and tris-NTA SAMs, respectively.

Structural Properties of Mixed MCH SAMs. Infrared spectroscopy provides further details on packing, conformation, and orientation of different moieties in mixed SAMs under investigation. The general observation seen in the spectra for the three mixed MCH SAMs is that the position of the CH stretching peaks is relatively stable upon increasing the mole fraction up to 30 mol %. The asymmetric stretch remains at 2918 cm^{-1}, and the FWHM value is also stable suggesting that the supporting layer of the alkyls is not disturbed by the presence of the MCHs

(33) Hederos, M.; Konradsson, P.; Borgh, A.; Liedberg, B. *J. Phys. Chem. B* **2005**, *109*, 15849−15859.
(34) Schaferling, M.; Riepl, M.; Pavlickova, P.; Paul, H.; Kambhampati, D.; Liedberg, B. *Microchim. Acta* **2003**, *142*, 193−203.

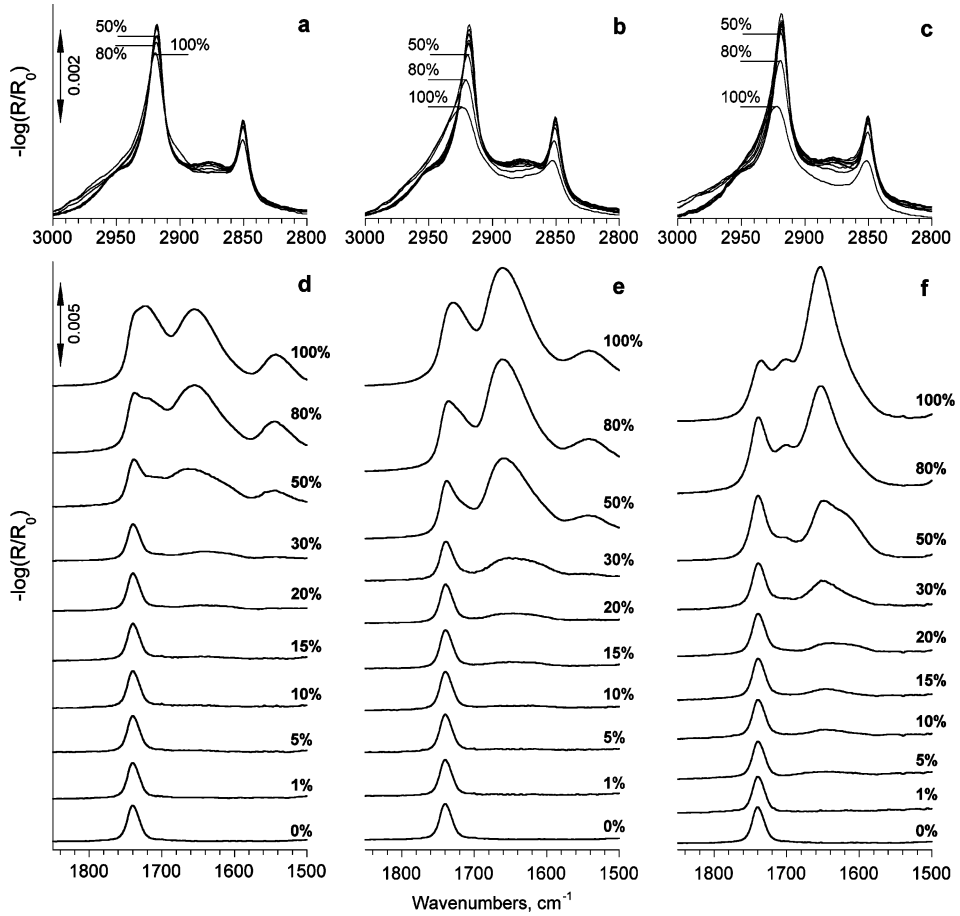

Figure 5. Left to right- infrared reflection−absorption spectra of mixed mono-, bis-, and tris-NTA SAMs. (a−c) the CH stretching region, and (d−f) a part of the fingerprint region between 1850 and 1500 cm^{-1}.

in the SAM. However, the alkyl peaks broaden significantly as the solution concentration is increased above 50 mol %. Such a broadening of alkyl peaks, as well as the distinctive shift toward higher frequencies, is, as mentioned before, characteristic of an increasing amount of gauche defects and loss of the overall conformational order of the alkyl layer.[33]

The most interesting information in the low-frequency region can be found by observing the NTA-related peaks between 1850 and 1500 cm^{-1}, Figure 5 d−f. The increasing intensity of the NTA-related peaks supports the main observations from the ellipsometric and contact angle measurements above; that is, the surface concentration of MCHs increases continuously with increasing mole fraction up to approximately 80 mol %. Further on, the intensities of the diagnostic NTA peaks ν(C═O) and $\nu_a(COO^-)$ suggest that ethanol as a solvent leads to a lower fraction of MCH thiols in the formed SAMs compared to acetonitrile and THF used in the study by Tinazli et al.[12] For example, the intensities obtained for mono-NTA and bis-NTA at 30 mol % (Figure 5d,e) are close to those in the spectra of SAMs previously prepared from 3 mol % solutions of these compounds in acetonitrile and THF, respectively. This is most likely due to the different solubilities of the molecules under investigation in different solvents.

On the basis of the above-mentioned findings, which confirm that the supporting alkyl layer appears intact for the SAMs at low mol % of the MCHs, we will further analyze only the spectra of the SAMs prepared in the concentration range 1−30 mol %. Figure 6 shows the evolution of the integrated peak intensities obtained in the spectral region 1745−1577 cm^{-1}, dominated primarily by the NTA carbonyl and carboxylate groups, after having subtracted the pure EG_3 SAM spectrum, 0 mol %, Figure 5. The integrated peak intensities indicate how the total amount of the NTA groups on the surface, which is qualitatively proportional to the number of carboxylic group in the molecule, is related to the mole fraction of the MCH in the incubation solution. Thus, assuming the same extinction coefficients and similar orientation of the NTA groups in all three MCH SAMs, the obtained stochiometric ratios of the constituent molecules in the SAMs turn out to be rather close for each mole fraction, although no statistical analysis was performed for these time-consuming IRAS measurements. It should be born in mind that the increasing structural complexity and the use of a different coupling chemistry of the three MCHs give rise to slight differences in the appearance of the spectral signatures in the

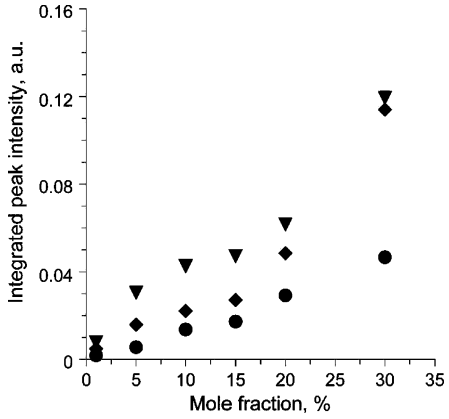

Figure 6. Comparison of the integrated NTA peak intensities for mono-NTA (circles), bis-NTA (diamonds), and tris-NTA (triangles). Integration interval was 1745−1577 cm^{-1}.

region between 1850 and 1500 cm^{-1}. For example, the integrated intensities obtained from the tris-NTA spectra contain contributions from the carbonyls of the linkage groups of the molecule. Thus, we stress that the IR intensity analysis in Figure 6 provides only a crude estimate of the relative amount of the MCHs, and for a careful determination of the surface concentrations, other analytical techniques should be used, e.g., XPS or isotope (S^{35}) labeling. It is also expected that the accuracy will decrease with increasing surface fraction of MCH group because of interfering in-plane interactions and concomitant spectral changes. To summarize, the above-discussed ellipsometric, contact angle, and IRAS measurements allow us to conclude that the SAMs prepared from solutions containing 0−30 mol % of the MCH thiols display a gradual variation in terms of chelator distribution. At the same time, the structure of the supporting alkyl and EG_3 matrix remains intact in this mole fraction range, a prerequisite for obtaining properly exposed MCHs to the ambient. The SAMs formed at high MCH mole fractions are less ordered, and, most likely, the MCH groups are experiencing stronger intermolelular interactions and steric constraints, which could affect their function as multivalent chelators. Therefore, we decided to prepare samples from solutions containing 0−30 mol % of the MCH thiols for an in-depth comparison of the His-tagged protein binding and elution characteristics.

Protein Binding Characteristics. The functional characteristics of mono-, bis-, and tris-NTA were investigated with SPR, Figure 7. Figure 7a shows the immobilization of ifnar2-His_6 and its interaction with the ligand IFNα2 on 3 and 30 mol % mono-, bis-, and tris-NTA SAMs. In the control experiments without chelated Ni(II) ions, much lower binding of ifnar2- His_6 was detected, confirming that the proteins are specifically tethered through Ni(II)-coordinated histidines. The transient background signal during injection of ifnar2-His_6 in the control experiments is due to the presence of 1 mM EDTA for removal of transition metal ion contaminants in this sample. The amount of immobilized ifnar2-His_6 under these conditions was less than 10% of the amount of protein immobilized in the presence on Ni(II) ions. Upon injection of the ligand IFNα2, strong binding to immobilized ifnar2-His_6 was observed, which is highly specific as confirmed by the control experiments. The signal amplitude observed for the ligand confirmed the functional integrity of the immobilized protein. Furthermore, the ligand binding kinetics was very similar to the kinetics obtained in previous experiments with this biological system,[12,27,35] which has been shown to be highly sensitive to the immobilization technique.[35] The different shape of the association and dissociation curves observed for 3 and 30 mol % surfaces is due to more pronounced mass transport limitation for the 30 mol % surface (with more ligand binding sites). A high concentration of imidazole (1 M) efficiently removed the proteins from all the surfaces, confirming Ni(II) ion-specific immobilization. Upon closer inspection of the sensorgrams for 3 mol % chelator thiol, it can be seen that the immobilization of ifnar2- His_6 is only stable for tris-NTA, while for mono- and bis-NTA surfaces, ifnar2-His_6 dissociates substantially (300−500 s). This is an effect of molecular multivalency,[6,11] and it nicely demonstrates the benefits of using tris-NTA in applications at low surface densities of NTA groups. At 30 mol % of the MCH thiols, stable binding is observed for all chelator heads, confirming further stabilization by surface multivalency, which increases with increasing surface concentration of the chelator heads.[14] Another interesting observation is that the present set of SAMs appears to bind less protein as compared to those reported by Tinazli et al.[12] The protein

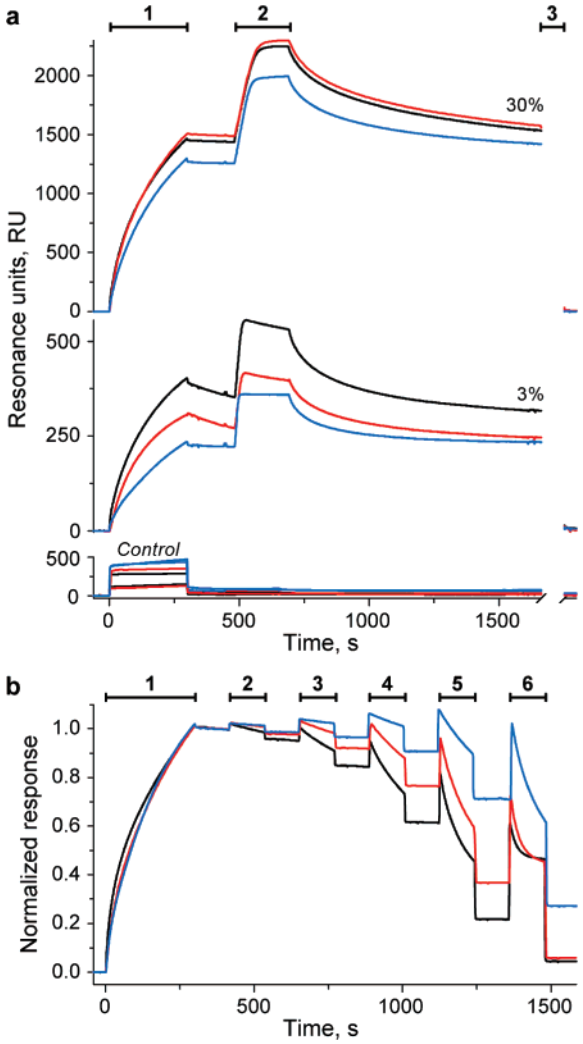

Figure 7. Functional demonstration of the multivalent chelator chips with SPR. a) Sensorgrams showing immobilization of 500 nM ifnar2-His_6 (1), followed by injection of 100 nM IFNα2 (2) and 1 mM imidazole (3) on surfaces of 30 mol % (top graph) and 3 mol % (middle graph) of mono-NTA (black line), bis-NTA (red line), and tris-NTA SAM (blue line). As a control experiment, the same sequence of samples were injected on the surfaces after removal of NTA-chelated Ni(II) ions with 200 mM EDTA (bottom graph). Note the different scaling of the *y*-axes. b) Elution of immobilized ifnar2-His_6 with increasing imidazole concentrations on 30 mol % mono-NTA (black line), bis-NTA (red line), and tris-NTA SAM (blue line). The surfaces were loaded with 500 nM ifnar2- His_6 (1), and imidazole concentrations were 2 mM (2), 5 mM (3), 10 mM (4), 20 mM (5), and 40 mM (6). The sensorgrams have been normalized to the maximum immobilization level.

immobilization levels for their 3% bis-NTA surface correspond roughly to the levels obtained for our 30% surface, while our 3% surface binds insignificant levels of proteins in comparison. The difference lies in the different solvents used for self-assembly. Here we have used ethanol instead of THF and acetonitrile, which certainly affects the amount of the MCHs on surface for a given mol % in solution (see the discussion above).

The contrast in binding affinity between the different chelator thiols and ifnar2- His_6 is shown in Figure 7b. In this experiment, ifnar2- His_6 was immobilized on 30 mol % mono-, bis-, and tris-NTA SAMs and thereafter eluted with increasing concentrations of imidazole (from 2 to 40 mM). A consistently increasing binding strength is observed with increasing multivalency of the chelators; mono-NTA is most sensitive to imidazole, followed by bis- and then tris-NTA.

(35) Piehler, J.; Schreiber, G. *Anal. Biochem.* **2001**, *289*, 173−186.

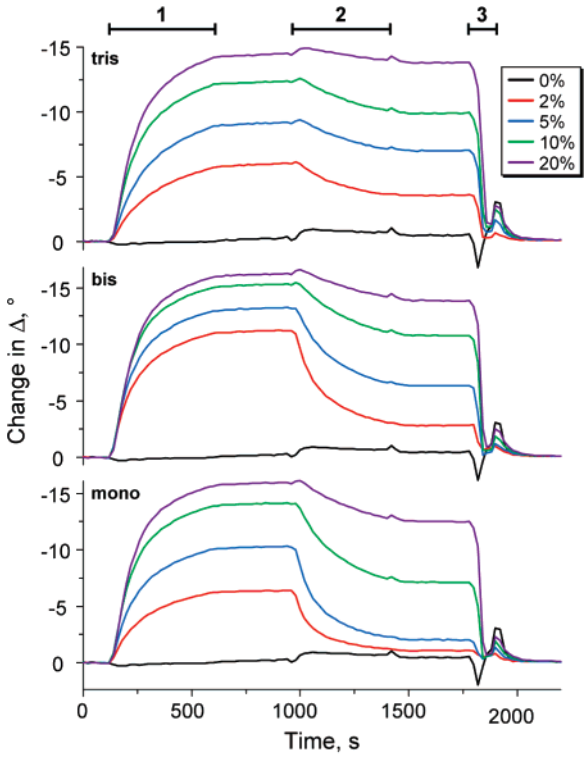

Figure 8. Kinetics measured by imaging surface plasmon resonance operated in ellipsometric mode showing immobilization of proteins on a density array obtained by dispensing mono-, bis-, and tris-NTA in four different mixing ratios with EG_3. The curves represent injection of (1) 500 nM MBP-His_{10}, (2) 60 mM imidazole, and (3) 0.5 M imidazole. The color coding for the different molar mixing ratios of chelator thiols is given in the legend.

For exploring the role of molecular and surface multivalency for protein immobilization, a 3 × 4 array consisting of 300 μm-sized spots was prepared as described by Klenkar et al.[13] Mono-, bis-, and tris-NTA was dispensed in three columns in four different mixing ratios (2, 5, 10, and 20 mol %) with EG_3.

For probing the binding stability, we used MBP fused to a His10-tag, which we have shown previously to be strongly affected by surface multivalency.[14] Figure 8 shows the binding of the MBP-His_{10} to the mono-, bis-, and tris- NTA spots (2, 5, 10, 20 mol %) and 1 control spot (0 mol %) followed by elution in imidazole at a low (60 mM) and regeneration at high concentration (0.5 M), respectively. The three MCH thiols, in all of the reported mixing ratios, are seen to bind the protein stably, as no dissociation is observed during buffer flow (note that a His_{10} tag is used this time[27]). The protein immobilization is also highly specific, as no adsorption is seen on the EG_3 control spot (0 mol %). As in the previous (non-array) experiment, a consistently decreasing protein elution is observed with increasing multivalency of the chelator thiols. The elution ranges from almost complete dissociation for 2 mol % of mono-NTA to hardly noticeable dissociation for 20 mol % of tris-NTA. In particular, tris-NTA displays a remarkable stability as compared to mono- and bis-NTA. Moreover, the gradual multivalency-dependent elution with imidazole can be used for protein multiplexing in microarray spots.[13,14] The same approach might be suitable to produce gradients in protein composition within the array via the controlled removal of the primary immobilized protein and subsequently introducing a second histidine-tagged protein. We are currently working on the analysis of protein−protein interactions, e.g., ternary complex formation, using MCH density arrays.

Conclusions

We have reported on the structural and functional properties of a series of complex self-assembled monolayers with terminal MCHs formed on gold from ethanol solutions. The work should be regarded as an extension of a previous of mono-NTA and bis-NTA SAMs.[12] In the present work, we introduced a new tris-NTA compound, studied, in detail, the SAM formation, and compared the subsequent protein binding/dissociation to/from the three different MCH SAMs as a function of surface composition.

We started by analyzing the influence of the bulky and complex MCHs, which contain charged and hydrogen bond accepting/donating groups, on the formation of single-component and mixed SAMs. Ellipsometry, water contact angle, and IRAS measurements confirm that the amount of the MCH groups on the surfaces increases with increasing mole fraction of the MCH thiols in the loading solution up to a critical mol % above which the surface concentration of MCH thiols start to decrease. Molar ratios 0−30 mol % of the MCH thiols with respect to the filling EG_3 molecule resulted in mixed MCH SAMs containing a densely packed alkyl layer, an amorphous ethylene glycol layer, and an outermost layer of MCH groups exposed to the ambient. Above 30 mol %, a significant degree of disorder is observed in the SAMs, making then less reliable for studies of His-tagged protein immobilization.

Our functional evaluation of the three NTA thiols revealed an increasing stability of the His-tagged proteins with increasing multivalency of the chelator head. The tris-NTA SAM displayed extraordinary stability of the ifnar2- His_6 receptor even at very low surface coverage of the MCH thiol molecules (prepared from 3 mol %). A high excess of Ni(II) ions on the surface, which is required for efficient immobilization through mono-NTA, strongly increases nonspecific binding of proteins. Thus, low-density tris-NTA SAMs provide a more selective capturing of proteins and detection of binding partners, which opens a range of applications in functional proteomics. Moreover, the chelator-dependent dissociation characteristics of immobilized His-tagged proteins offer a convenient tool for studies of complex multiprotein interactions at solid surfaces, and we foresee future applications in advanced biosensors and high throughput screening devices.

Acknowledgment. We acknowledge Gerhard Spatz-Kümbel (Institute of Biochemistry, Goethe-University Frankfurt) for excellent technical assistance. This research was supported by the Wallenberg Consortium North (WCN), the Swedish Research Council (VR), and the Swedish Foundation for Strategic Research (SSF) through the Biomimetic Materials Science program. This work was also supported by the German Research Council (DFG, Pi-405/1, Pi-405/2, and Ta-157/6) and by the German Ministry of Education and Research (BMBF, 0312005A). R.V. acknowledges the support from the Lithuanian State Science and Studies Foundation and the Swedish Institute through the Visby program.

Supporting Information Available: Full fingerprint region of infrared reflection−absorption spectra of mixed MCH and EG_3 SAMs shown in Figure 5. This information is available free of charge via the Internet at http://pubs.acs.org.

LA703709A